Strojnícky časopis – *Journal of* MECHANICAL ENGINEERING,
VOL 69 (2019), NO 2, 97 - 110

STOCHASTIC LOADING OF A SITTING HUMAN

FRYDRÝŠEK Karel[1], ČEPICA Daniel[1], HALO Tomáš[1]

[1]VŠB – Technical University of Ostrava, Faculty of Mechanical Engineering, Department of Applied Mechanics, 17. listopadu 2172/15. 708 00 Ostrava, Czech Republic, e-mail: karel.frydrysek@vsb.cz

Abstract: The aim of this paper is the biomechanical evaluation of the interaction between load forces to which a sitting man and the seat are exposed. All loads, which consider actual anthropometry histograms of human population (i.e. segmentation of human weight, height, centroids, gravity and shape of seat) are determined using the direct Monte Carlo Method. All inputs are based on the theory of probability (i.e. random/probabilistic inputs and outputs with respect their variabilities). A simple plane model (i.e. probabilistic normal forces and bending moments) shows a sufficient stochastic/probabilistic evaluation connected with biomechanics, ergonomics, medical engineering (implants, rehabilitation, traumatology, orthopaedics, surgery etc.) or industrial design.

KEYWORDS: Biomechanics, sitting man, seat, anthropometry, human segmentation, loadings, stochastics, probability, Monte Carlo Method.

1 Introduction

Sitting can be source of medical problems, e.g. influencing or even causing injuries or deformities in spine or in dorsum in general (i.e. oedema, hyperplasia, dermatitis, Secretan's syndrome, Scheuermann's disease, scoliosis, etc.). Treatment of dorsal back pains or diseases is quite often and it is usually “optimally” directed toward a diagnosed or suspected specific cause (see Fig. 1).

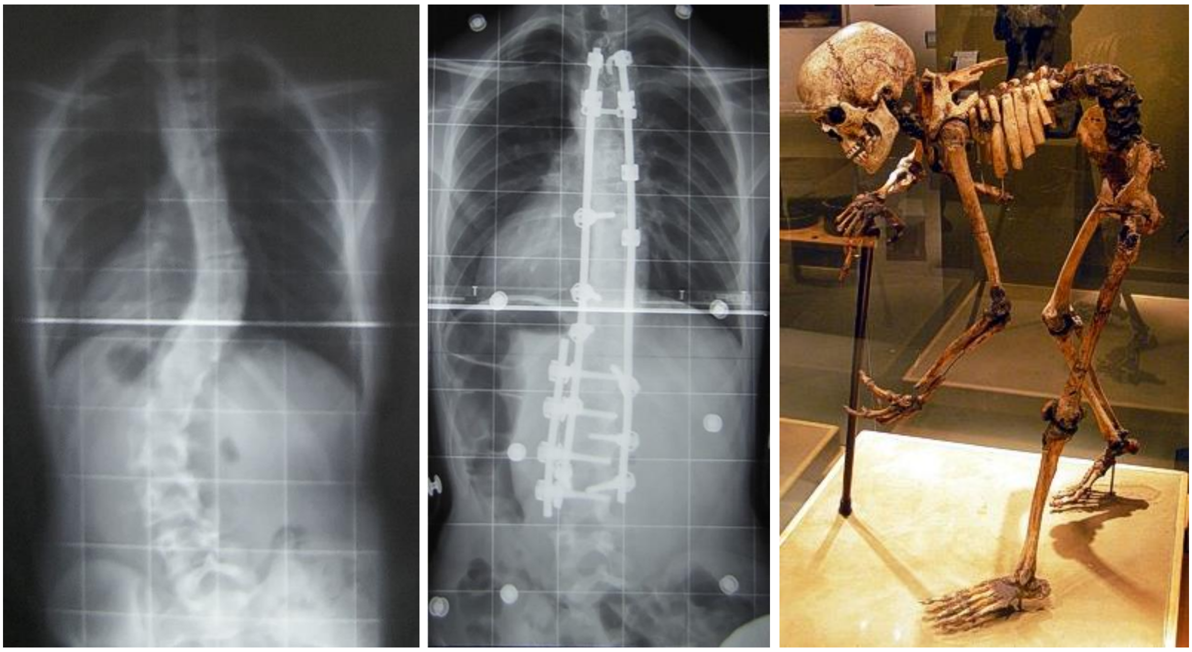

Fig. 1 X-ray snapshot of a human with lumbar dextroscoliosis and thoracic levoscoliosis (a) preoperative, (b) postoperative; (c) archeology – a middle ages women with severe scoliosis (Limburgs Museum, Venlo, The Nederlands).

DOI: 10.2478/scjme-2019-0020, Print ISSN 0039-2472, On-line ISSN 2450-5471

Human scoliosis (i.e. abnormal sideways curve/curves of spine) generally firstly occurs in children, when they experience their growth spurt. However, it can occur at other ages if it's caused by something else like a muscle disease, such as muscular atrophy, cerebral palsy, old age etc.

To analyze loads acting on a sitting human, a simple and easy to apply model was created. Stochastic (i.e. fully probabilistic) approach is used to take the real variety of human population into account. The probabilistic evaluation is done using direct Monte Carlo Method – random simulations (generated results) restricted by given variable inputs, where the inputs are chosen according to the real (measured or published) anthropometric parameters, different shapes of chair and location on Earth.

Application of probabilistic approaches is a new and modern trend in science research and development; see reference [3] to [9], [12], [13].

2 Model of Sitting Human – Normal/Reaction Forces and Bending Moments

In mechanics and engineering approach, truss structures appear to be the easiest ways of introducing, explaining and solving geometrical and material linearities or nonlinearities; see Fig. 2 and reference [10] and [11]. However, truss structures can be easy applied in biomechanics too; see the following text.

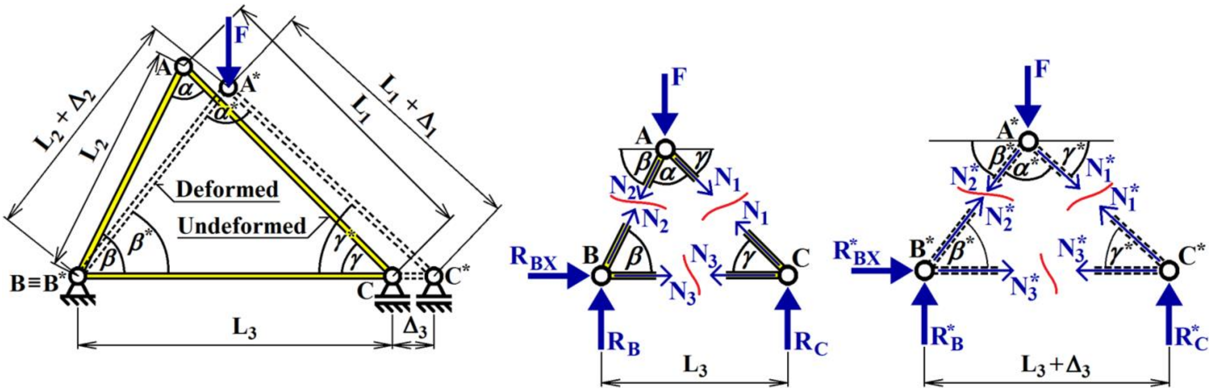

Fig. 2 Example of truss structure loaded by vertical force F - (a) general description, (b) solution according to the theory of 1st order (Method of Joints), (c) solution according to the theory of 2nd order (Method of Joints)

In the following text, the theory of 1st order is applied (i.e. fully linear model).

Simple (2D, plane) model of a sitting human (see Fig. 3 and 4), similar to truss structure, is constructed from 4 segments (segment $\boxed{1}$ – feet and legs, segment $\boxed{2}$ – thighs, segment $\boxed{3}$ – lower part of torso, segment $\boxed{4}$ – upper part of torso and head with neck) and 5 joints (A – E) (see Fig. 3 and 4). Gravitational forces acting in centroids (see Fig. 4a) are distributed to adjacent joints too (see Fig. 4b and 5). Model was derived by using the Method of Joints.

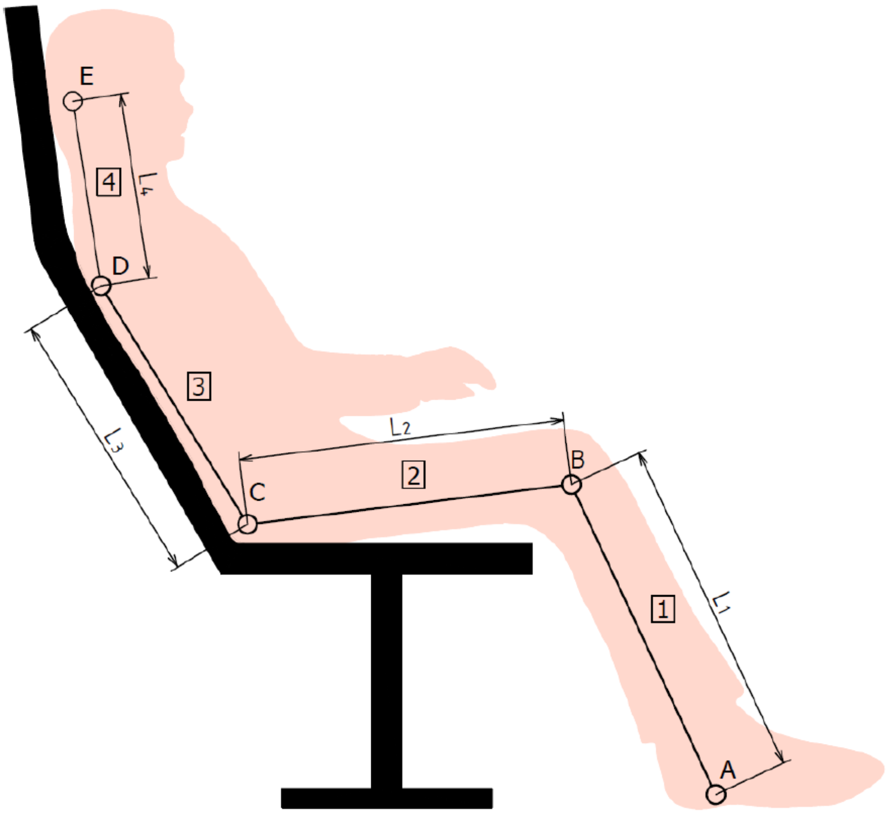

Fig. 3 Sitting human

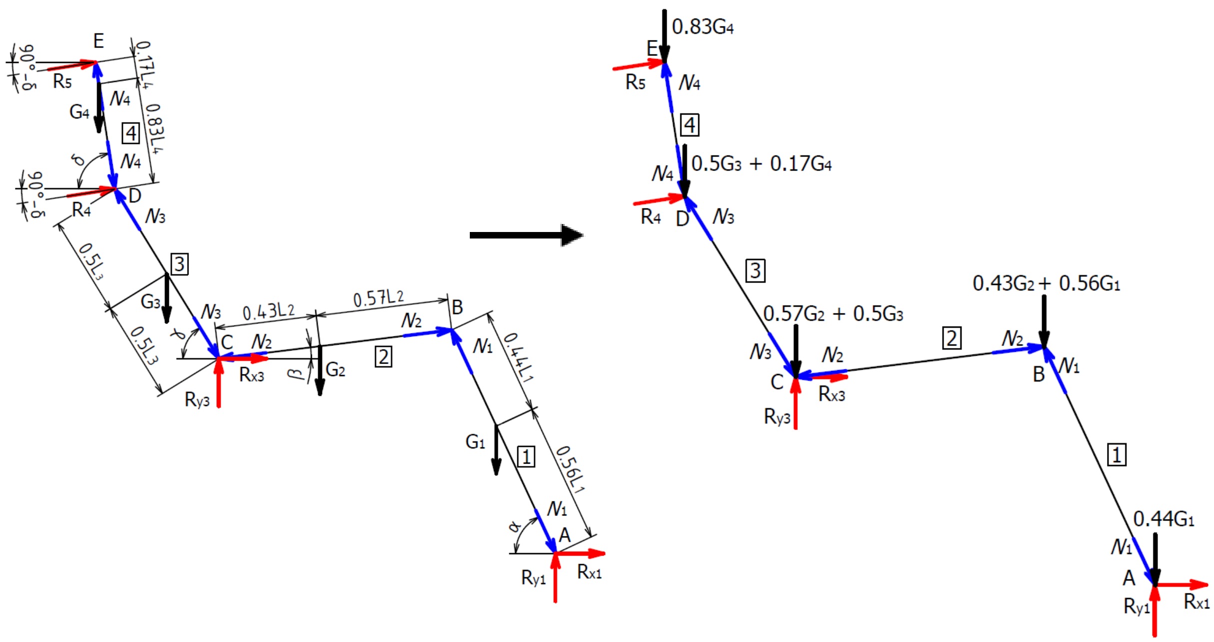

Fig. 4 Model of a sitting man as a biomechanical truss structure

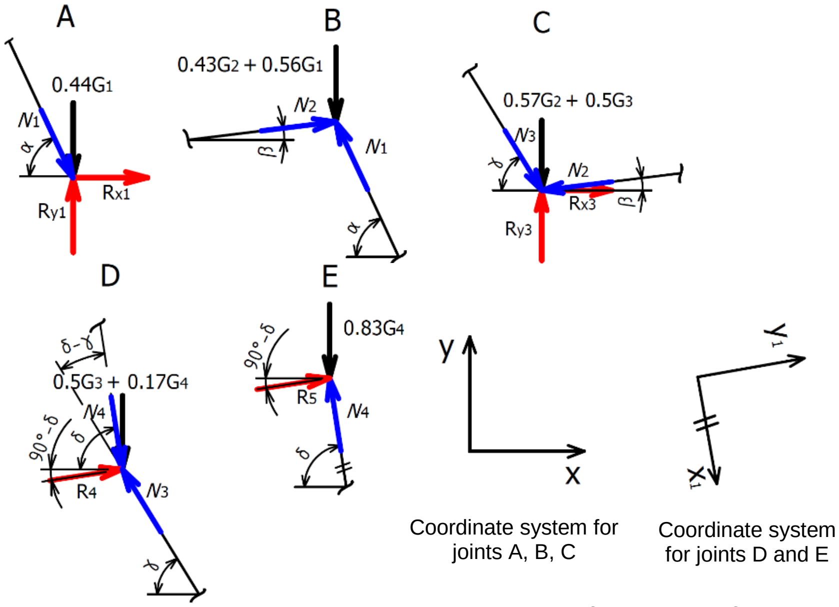

Fig. 5 Free body diagrams (application of Method of Joints)

2.1 Normal and Reaction Forces

Derivations of reaction forces and normal (internal) forces are very important for biomechanics of a sitting human or design of a seat.

From equilibrium equations of each joint (see Fig. 5), the final formulae of reaction R_j [N] and normal forces N_i [N] (in Fig. 5, the chosen orientations represent pressure) were derived; see eq. (1) to (10).

$$N_1 = \frac{(0.56 \cdot G_1 + 0.43 \cdot G_2) \cdot \cos(\beta)}{\sin(\alpha + \beta)} \tag{1}$$

$$N_2 = \frac{(0.56 \cdot G_1 + 0.43 \cdot G_2) \cdot \cos(\alpha)}{\sin(\alpha + \beta)} \tag{2}$$

$$N_3 = \frac{[0.5 \cdot G_3 + G_4] \cdot \sin(\delta)}{\cos(\delta - \gamma)} \tag{3}$$

$$N_4 = 0.83 \cdot G_4 \cdot \sin(\delta) \tag{4}$$

$$R_{x1} = -\frac{(0.56 \cdot G_1 + 0.43 \cdot G_2) \cdot \cos(\beta) \cdot \cos(\alpha)}{\sin(\alpha + \beta)} \tag{5}$$

$$R_{y1} = 0.43 \cdot G_1 + \frac{(0.56 \cdot G_1 + 0.43 \cdot G_2) \cdot \cos(\beta) \cdot \sin(\alpha)}{\sin(\alpha + \beta)} \tag{6}$$

$$\begin{aligned} R_{x3} = &-\frac{[0.5 \cdot G_3 \cdot \sin(\delta) + G_4 \cdot \sin(\delta)] \cdot \cos(\gamma)}{\cos(\delta - \gamma)} + \\ &+ \frac{(0.56 \cdot G_1 + 0.43 \cdot G_2) \cdot \cos(\alpha) \cdot \cos(\beta)}{\sin(\alpha + \beta)} \end{aligned} \tag{7}$$

$$\begin{aligned} R_{y3} = 0.57 \cdot G_2 + 0.5 \cdot G_3 &+ \frac{(0.56 \cdot G_1 + 0.43 \cdot G_2) \cdot \cos(\alpha) \cdot \sin(\beta)}{\sin(\alpha + \beta)} + \\ &+ \frac{[0.5 \cdot G_3 + G_4] \cdot \sin(\delta) \cdot \sin(\gamma)}{\cos(\delta - \gamma)} \end{aligned} \tag{8}$$

$$R_4 = 0.5 \cdot G_3 \cdot \cos(\delta) + 0.17 \cdot G_4 \cdot \cos(\delta) + \frac{[0.5 \cdot G_3 + G_4 \cdot] \cdot \sin(\delta) \cdot \sin(\delta - \gamma)}{\cos(\delta - \gamma)} \tag{9}$$

$$R_5 = 0.83 \cdot G_4 \cdot \cos(\delta) \tag{10}$$

2.2 Bending Moments

Derivations of bending (internal) moments are very important for biomechanics of a sitting human or design of a seat.

To determine bending moments, forces acting outside of joints must be considered – in this case we can calculate the moments the same way we would on an angled beam; see eq. (11) to (18).

Segment $\boxed{1}$: $z_1 \in< 0; 0.56 \cdot L_1 >, z_2 \in< 0; 0.44 \cdot L_1 >$

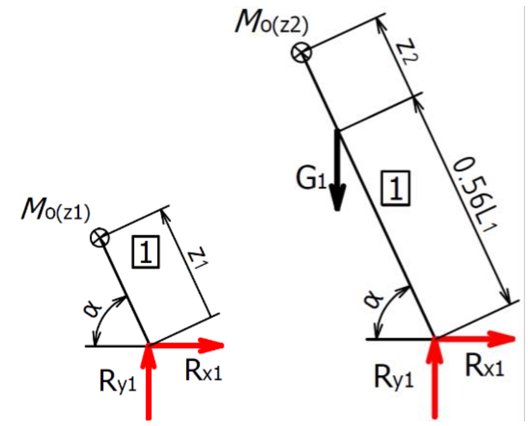

Fig. 6 Segment $\boxed{1}$

$$M_{o(z1)} = R_{y1} \cdot z_1 \cdot \cos(\alpha) + R_{x1} \cdot z_1 \cdot \sin(\alpha) \tag{11}$$

$$\begin{gathered} M_{o(z2)} = R_{y1} \cdot (z_2 + 0.56 \cdot L_1) \cdot \cos(\alpha) + R_{x1} \cdot (z_2 + 0.56 \cdot L_1) \cdot \sin(\alpha) + \\ -G_1 \cdot z_2 \cdot \cos(\alpha) \end{gathered} \tag{12}$$

Segment $\boxed{2}$: $z_3 \in< 0; 0.57 \cdot L_2 >, z_4 \in< 0; 0.43 \cdot L_2 >$

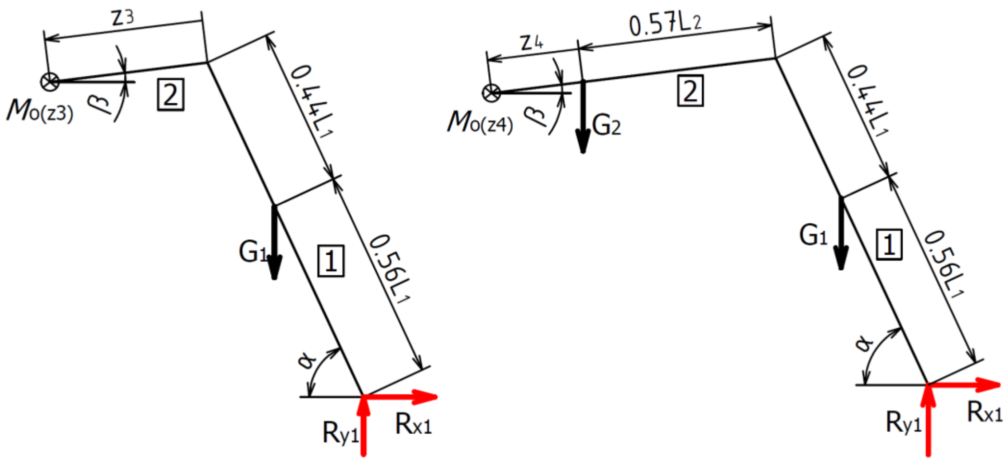

Fig. 7 Segment $\boxed{2}$

$$\begin{gathered} M_{o(z3)} = R_{y1} \cdot (L_1 \cdot \cos(\alpha) + z_3 \cdot \cos(\beta)) + R_{x1} \cdot (L_1 \cdot \sin(\alpha) - z_3 \cdot \sin(\beta)) + \\ -G_1 \cdot \big(0.43 \cdot L_1 \cdot \cos(\alpha) + z_3 \cdot \cos(\beta)\big) \end{gathered} \tag{13}$$

$$\begin{gathered} M_{o(z4)} = R_{y1} \cdot (L_1 \cdot \cos(\alpha) + (z_4 + 0.57 \cdot L_2) \cdot \cos(\beta)) + \\ +R_{x1} \cdot (L_1 \cdot \sin(\alpha) - (z_4 + 0.57 \cdot L_2) \cdot \sin(\beta)) + \\ -G_1 \cdot \big(0.44 \cdot L_1 \cdot \cos(\alpha) + (z_4 + 0.57 \cdot L_2) \cdot \cos(\beta)\big) - G_2 \cdot z_4 \cdot \cos(\beta) \end{gathered} \tag{14}$$

Segment $\boxed{4}$: $z_5 \in <0; 0.17 \cdot L_4>, z_6 \in <0; 0.83 \cdot L_4>$

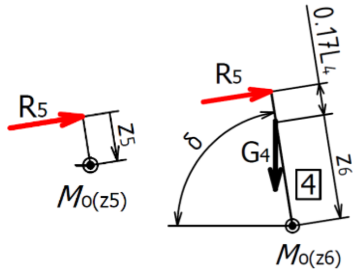

Fig. 8 Segment $\boxed{4}$

$$M_{o(z5)} = R_5 \cdot z_5 \tag{15}$$
$$M_{o(z6)} = R_5 \cdot (z_6 + 0.17 \cdot L_4) - G_4 \cdot z_6 \cdot \cos(\delta) \tag{16}$$

Segment $\boxed{3}$: $z_7 \in <0; 0.5 \cdot L_3>, z_8 \in <0; 0.5 \cdot L_3>$

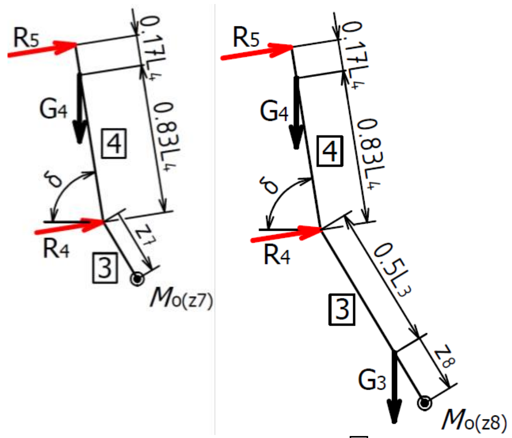

Fig. 9 Segment $\boxed{3}$

$$\begin{gathered} M_{o(z7)} = R_5 \cdot \cos(\delta) \cdot (L_4 \cdot \cos(\delta) + z_7 \cdot \cos(\gamma)) + \\ +R_5 \cdot \sin(\delta) \cdot (L_4 \cdot \sin(\delta) + z_7 \cdot \sin(\gamma)) + \\ +R_4 \cdot \cos(\delta) \cdot z_7 \cdot \cos(\gamma) + R_4 \cdot \sin(\delta) \cdot z_7 \cdot \sin(\gamma) + \\ -G_4 \cdot (0.83 \cdot L_4 \cdot \cos(\delta) + z_7 \cdot \cos(\gamma)) \end{gathered} \tag{17}$$

$$\begin{gathered} M_{o(z8)} = R_5 \cdot \cos(\delta) \cdot (L_4 \cdot \cos(\delta) + (z_8 + 0.5 \cdot L_3) \cdot \cos(\gamma)) + \\ +R_5 \cdot \sin(\delta) \cdot (L_4 \cdot \sin(\delta) + (z_8 + 0.5 \cdot L_3) \cdot \sin(\gamma)) + \\ +R_4 \cdot \cos(\delta) \cdot (z_8 + 0.5 \cdot L_3) \cdot \cos(\gamma) + \\ +R_4 \cdot \sin(\delta) \cdot (z_8 + 0.5 \cdot L_3) \cdot \sin(\gamma) + \\ -G_4 \cdot (0.83 \cdot L_4 \cdot \cos(\delta) + z_8 \cdot \cos(\gamma)) - G_3 \cdot z_8 \cdot \cos(\gamma). \end{gathered} \tag{18}$$

Maximum bending moments are in centroids of each segment; see eq. (19) to (22).

$$M_{omax1} = R_{y1} \cdot 0.56 \cdot L_1 \cdot \cos(\alpha) + R_{x1} \cdot 0.56 \cdot L_1 \cdot \sin(\alpha) \tag{19}$$

$$\begin{gathered} M_{omax2} = R_{y1} \cdot (L_1 \cdot \cos(\alpha) + 0.57 \cdot L_2 \cdot \cos(\beta)) + \\ +R_{x1} \cdot (L_1 \cdot \sin(\alpha) - 0.57 \cdot L_2 \cdot \sin(\beta)) - G_1 \cdot (0.44 \cdot L_1 \cdot \cos(\alpha)) + \\ +0.57 \cdot L_2 \cdot \cos(\beta) \end{gathered} \tag{20}$$

$$\begin{gathered} M_{omax3} = -G_4 \cdot (0.83 \cdot L_4 \cdot \cos(\delta) + 0.5 \cdot L_3 \cdot \cos(\gamma)) + \\ +R_5 \cdot \sin(\delta) \cdot (L_4 \cdot \sin(\delta) + 0.5 \cdot L_3 \cdot \sin(\gamma)) + \\ +R_4 \cdot \cos(\delta) \cdot 0.5 \cdot L_3 \cdot \cos(\gamma) + R_4 \cdot \sin(\delta) \cdot 0.5 \cdot L_3 \cdot \sin(\gamma) + \\ +R_5 \cdot \cos(\delta) \cdot (L_4 \cdot \cos(\delta) + 0.5 \cdot L_3 \cdot \cos(\gamma)) \end{gathered} \tag{21}$$

$$M_{omax4} = R_5 \cdot 0.17 \cdot L_4 \tag{22}$$

3 Example of Normal Forces Diagram and Bending Moments Diagram

Normal forces diagram is presented in Fig. 10 (a) and bending moment diagram is presented in Fig. 10 (b).

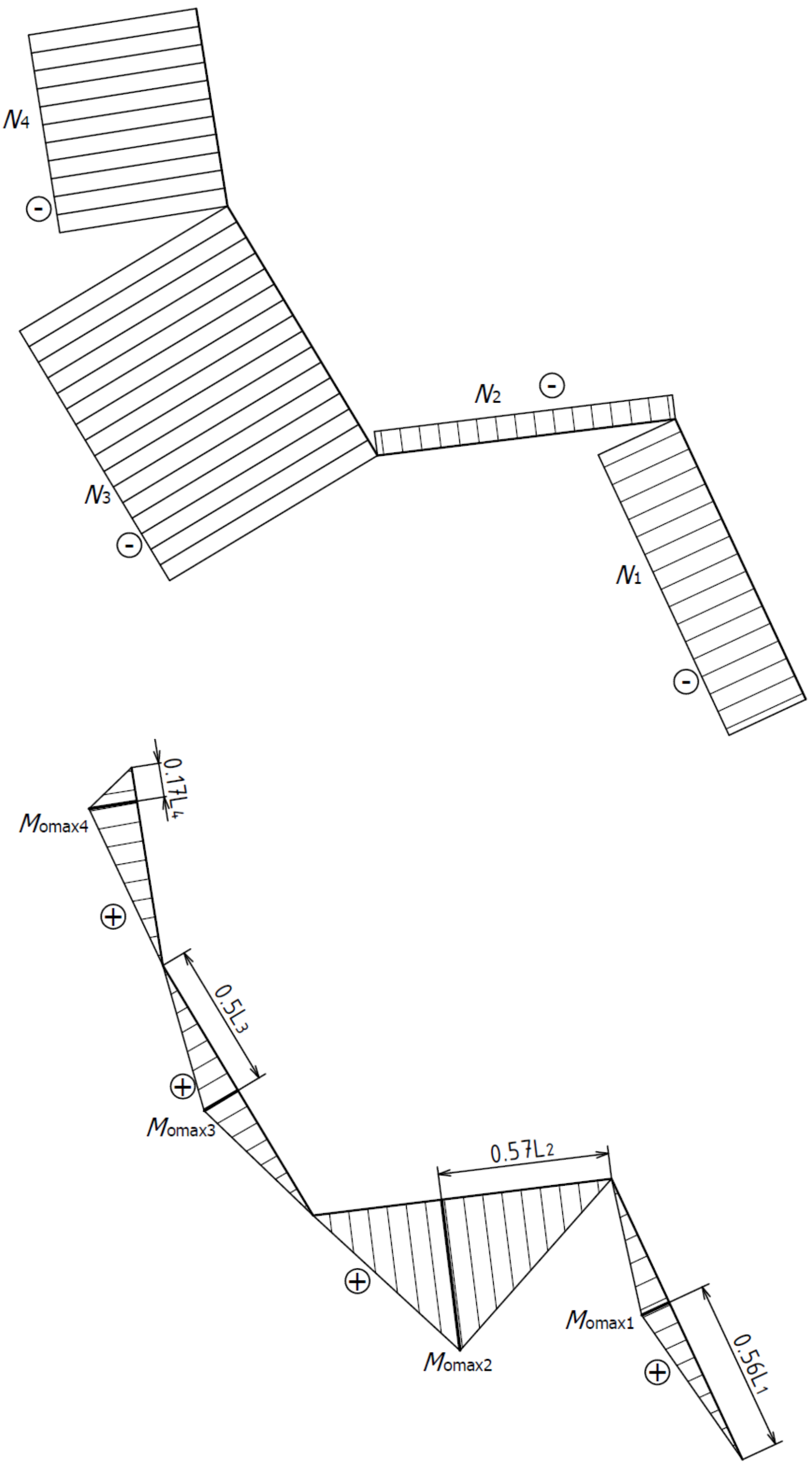

Fig. 10 (a) Normal forces diagram – Example of sitting human evaluation, (b) Bending moments diagram – Example of sitting human evaluation

4 Stochastic/Probabilistic Inputs and Outputs

All the data are described via histograms with truncated (bounded) normal distribution. Histograms of total height and weight are given by references [1] and [2], gravitational acceleration g is given by location on Earth. Segment angles α, β and δ were chosen (depends on design of chair). Angle γ is related to δ (see Tab. 1) to avoid unrealistic results. Lengths and weights of segments are functions of total height/weight.

Output data are calculated in Anthill software 2.6 Pro (direct Monte Carlo Method) using 10^7 random simulations for very accurate results.

Inputs:

Tab. 1 Input data (human anthropometry, design of a seat and Earth's gravity)

Variable name		Symbol	Min. value	Mean value	Median value	Max. value	Graph
Total weight [kg]		m	45	89.998	89.951	135	Graph 1
Total height [m]		h	1.2	1.8	1.8	2.4	Graph 2
Angle of segment $\boxed{1}$ [deg]		α	60	74.998	74.991	90	Graph 3
Angle of segment $\boxed{2}$ [deg]		β	0	9.998	9.981	20	Graph 4
Angle of segment $\boxed{3}$ [deg]		$\gamma = \frac{14}{15} \cdot \delta$	60.67	69.999	69.988	79.33	Graph 5
Angle of segment $\boxed{4}$ [deg]		δ	65	74.999	74.987	85	Graph 6
Gravitational acc. [m/s^2]		g	9.78	9.806	9.806	9.832	Graph 7
Length [m]	Segment $\boxed{1}$	$L_1 = 0.285 \cdot h$	0.342	0.513	0.512	0.684	Graph 8
	Segment $\boxed{2}$	$L_2 = 0.245 \cdot h$	0.294	0.441	0.441	0.588	Graph 9
	Segment $\boxed{3}$	$L_3 = 0.24 \cdot h$	0.288	0.432	0.432	0.576	Graph 10
	Segment $\boxed{4}$	$L_4 = 0.165 \cdot h$	0.198	0.297	0.297	0.396	Graph 11
Weight [kg]	Segment $\boxed{1}$	$m_1 = 0.124 \cdot m$	5.58	11.158	11.138	16.74	Graph 12
	Segment $\boxed{2}$	$m_2 = 0.248 \cdot m$	11.16	22.317	22.275	33.48	Graph 13
	Segment $\boxed{3}$	$m_3 = 0.4 \cdot m$	18	35.996	35.928	54	Graph 14
	Segment $\boxed{4}$	$m_4 = 0.228 \cdot m$	10.26	20.518	20.479	30.78	Graph 15
Gravit. force [N]	Segment $\boxed{1}$	G_1	54.58	109.429	109.435	164.567	Graph 16
	Segment $\boxed{2}$	G_2	109.161	218.859	218.87	329.134	Graph 17
	Segment $\boxed{3}$	G_3	176.066	352.998	353.016	530.862	Graph 18
	Segment $\boxed{4}$	G_4	100.357	201.209	201.219	302.591	Graph 19

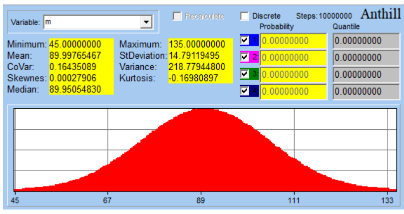

Graph 1 Total weight
m ∈ ⟨45; 135⟩ kg

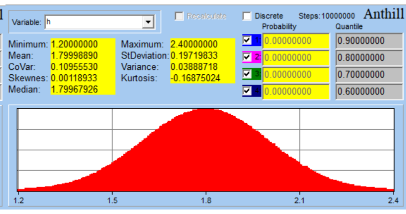

Graph 2 Total height
h ∈ ⟨1.2; 135⟩ m

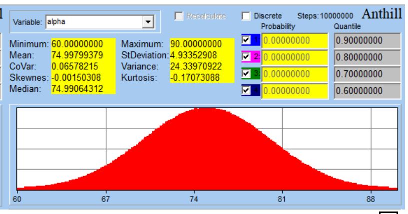

Graph 3 Angle – segment $\boxed{1}$
$\alpha \in \langle 60; 90\rangle$ deg

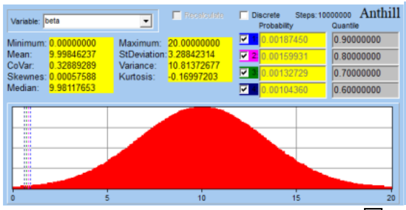

Graph 4 Angle –segment $\boxed{2}$
$\beta \in \langle 0; 20)$ deg

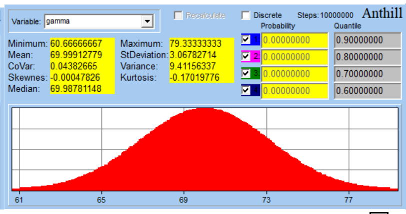

Graph 5 Angle – segment $\boxed{3}$
$\gamma \in \langle 60.67; 79.33\rangle$ deg

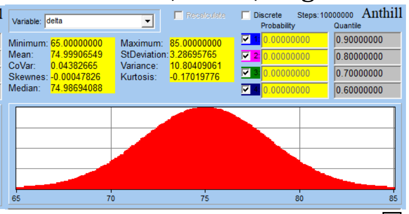

Graph 6 Angle – segment $\boxed{4}$
$\delta \in \langle 65; 85\rangle$ deg

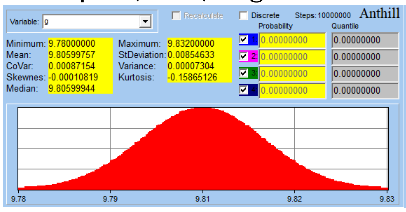

Graph 7 Gravitational acc.
$g \in \langle 9.78; 9.832\rangle$ m/s^2

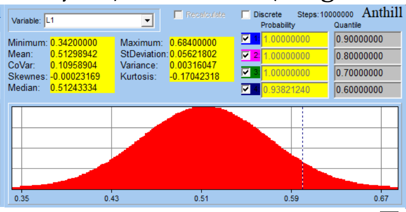

Graph 8 Length – segment $\boxed{1}$
$L_1 \in \langle 0.342; 0.684\rangle$ m

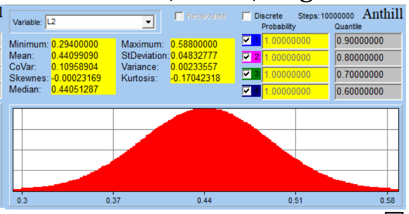

Graph 9 Length – segment $\boxed{2}$
$L_2 \in \langle 0.294; 0.588\rangle$ m

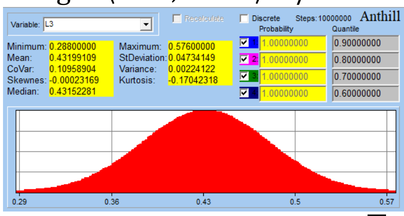

Graph 10 Length – segment $\boxed{3}$
$L_3 \in \langle 0.288; 0.576\rangle$ m

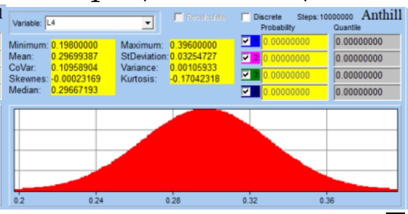

Graph 11 Length – segment $\boxed{4}$
$L_4 \in \langle 0.198; 0.396\rangle$ m

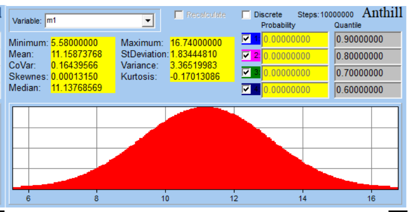

Graph 12 Weight – segment $\boxed{1}$
$m_1 \in \langle 5.58; 16.74\rangle$ kg

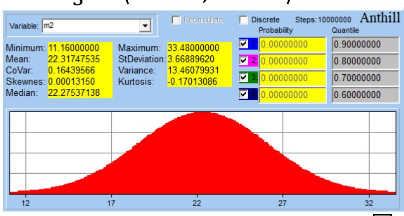

Graph 13 Weight – segment $\boxed{2}$
$m_2 \in \langle 11.16; 33.48\rangle$ kg

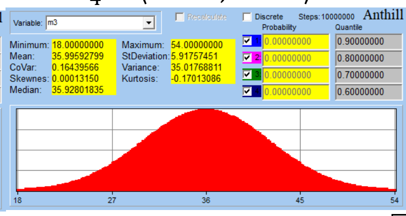

Graph 14 Weight – segment $\boxed{3}$
$m_3 \in \langle 18; 54\rangle$ kg

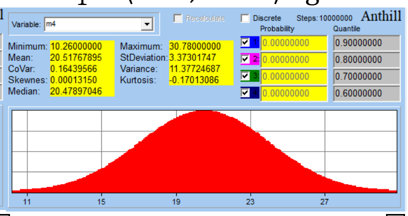

Graph 15 Weight – segment $\boxed{4}$
$m_4 \in \langle 10.26; 30.78\rangle$ kg

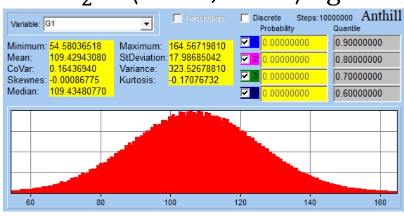

Graph 16 G. force – segment $\boxed{1}$
$G_1 \in \langle 54.58; 164.567\rangle$ N

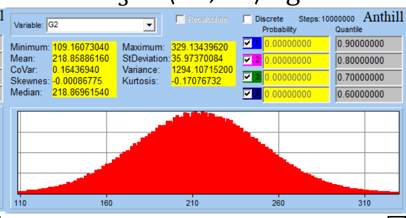

Graph 17 G. force – segment $\boxed{2}$
$G_2 \in \langle 109.161; 329.134\rangle$ N

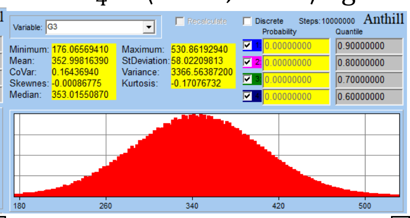

Graph 18 G. force – segment $\boxed{3}$
$G_3 \in \langle 176.066; 530.862\rangle$ N

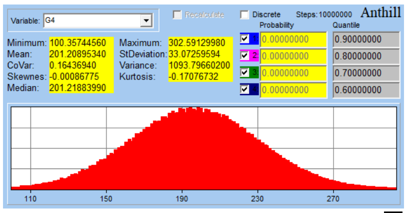

Graph 19 G. force – segment $\boxed{4}$

$G_4 \in \langle 100.357; 302.591 \rangle$ N

Note: The sum of all lengths of segments is smaller than total height (i.e. $\sum_1^4 L_i < h$). The reason is, the head is propped on chair in half of its length; see Fig. 3 and 4.

Outputs:

Tab. 2 Output data (calculated normal and reaction forces and bending moments)

Variable name		Symbol	Min. value	Mean value	Median value	Max. value	Graph
Internal normal force [N]	Segment $\boxed{1}$	N_1	73.367	154.2	154.145	262.296	Graph 20
	Segment $\boxed{2}$	N_2	0	40.535	39.554	128.811	Graph 21
	Segment $\boxed{3}$	N_3	172.652	365.611	365.535	566.686	Graph 22
	Segment $\boxed{4}$	N_4	76.115	161.038	161.006	249.36	Graph 23
Reaction force [N]	Feet – X direction	R_{x1}	-128.809	-39.856	-38.879	0	Graph 24
	Feet – Y direction	R_{y1}	91.425	196.529	196.475	305.431	Graph 25
	Buttock – X direction	R_{x3}	-240.59	-84.724	-83.425	12.204	Graph 26
	Buttock – Y direction	R_{y3}	305.726	651.419	651.192	1029.748	Graph 27
	Dorsum	R_4	28.091	86.332	85.601	172.559	Graph 28
	Head	R_5	7.546	43.15	42.456	105.244	Graph 29
Max. internal bending moment [Nm]	Segment $\boxed{1}$	M_{OMAX1}	0	3.566	3.464	12.567	Graph 30
	Segment $\boxed{2}$	M_{OMAX2}	7.796	23.257	23.058	46.975	Graph 31
	Segment $\boxed{3}$	M_{OMAX3}	3.011	13.02	12.771	34.983	Graph 32
	Segment $\boxed{4}$	M_{OMAX4}	0.324	2.179	2.126	6.63	Graph 33

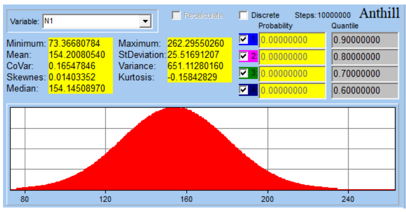

Graph 20 N. force – segment $\boxed{1}$
$N_1 \in \langle 73.367; 262.296\rangle$ N

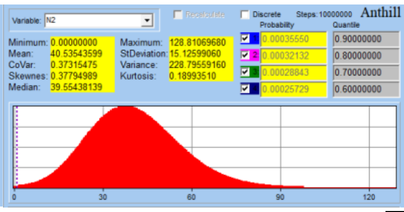

Graph 21 N. force – segment $\boxed{2}$
$N_2 \in \langle 0; 128.811\rangle$ N

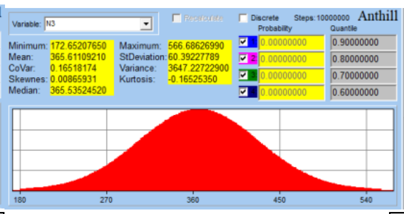

Graph 22 N. force – segment $\boxed{3}$
$N_3 \in \langle 172.652; 566.683\rangle$ N

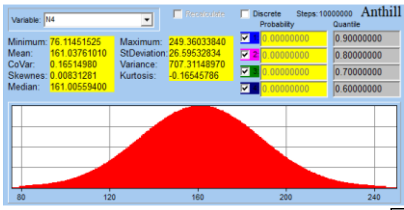

Graph 23 N. force – segment $\boxed{4}$
$N_4 \in \langle 76.115; 249.36\rangle$ N

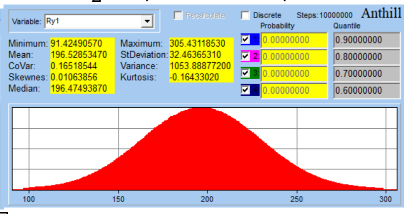

Graph 24 R. force – foot (X)
$\mathrm{R}_{y1} \in \langle 91.425; 305.431\rangle$ N

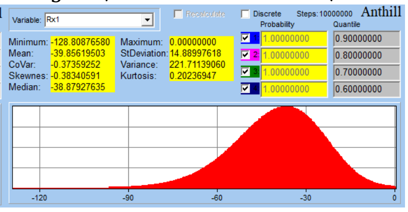

Graph 25 R. force – foot (Y)
$\mathrm{R}_{x1} \in \langle -128.809; 0\rangle$ N

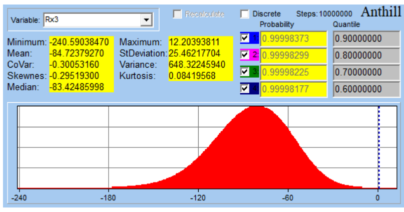

Graph 26 R. force – buttock (X)
$\mathrm{R}_{x3} \in \langle -240.59; 12.204\rangle$ N

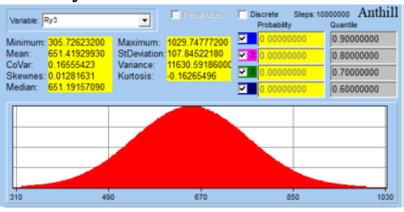

Graph 27 R. force – buttock (Y)
$\mathrm{R}_{y3} \in \langle 305.726; 1029.748\rangle$ N

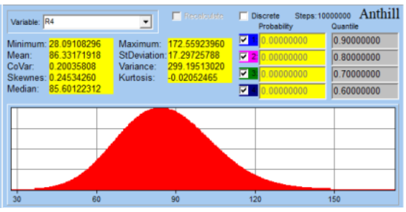

Graph 28 R. force – dorsum
$\mathrm{R}_4 \in \langle 28.091; 172.559\rangle$ N

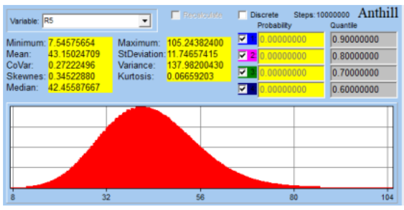

Graph 29 R. force – head
$\mathrm{R}_5 \in \langle 7.546; 105.244\rangle$ N

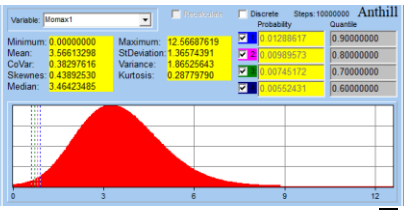

Graph 30 Moment – segment $\boxed{1}$
$M_{\mathrm{OMAX1}} \in \langle 0; 12.567\rangle$ Nm

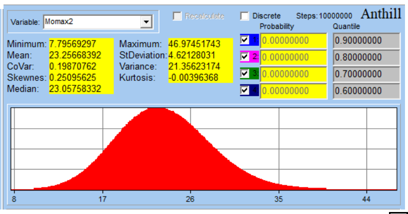

Graph 31 Moment – segment $\boxed{2}$
$M_{\mathrm{OMAX2}} \in \langle 7.796; 46.975\rangle$ Nm

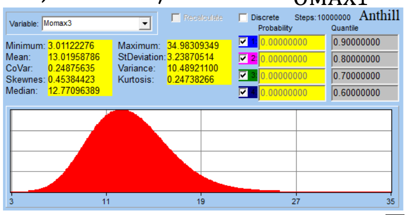

Graph 32 Moment – segment $\boxed{3}$
$M_{\mathrm{OMAX3}} \in \langle 3.011; 34.983\rangle$ Nm

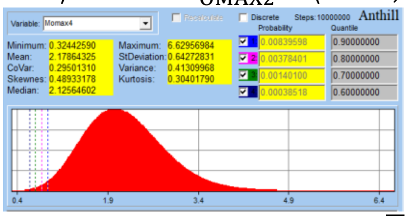

Graph 33 Moment – segment $\boxed{4}$
$M_{\mathrm{OMAX4}} \in \langle 0.324; 6.63\rangle$ Nm

In some output histograms we can see skewness/kurtosis of histograms. This is OK and it is caused by combination of mathematical and statistical operations.

5 Probabilistic Diagram of Normal Forces and Bending Moments

By putting the histograms of normal forces and bending moments into diagrams we can better visualize the range of normal forces and bending moments that are acting in segments.

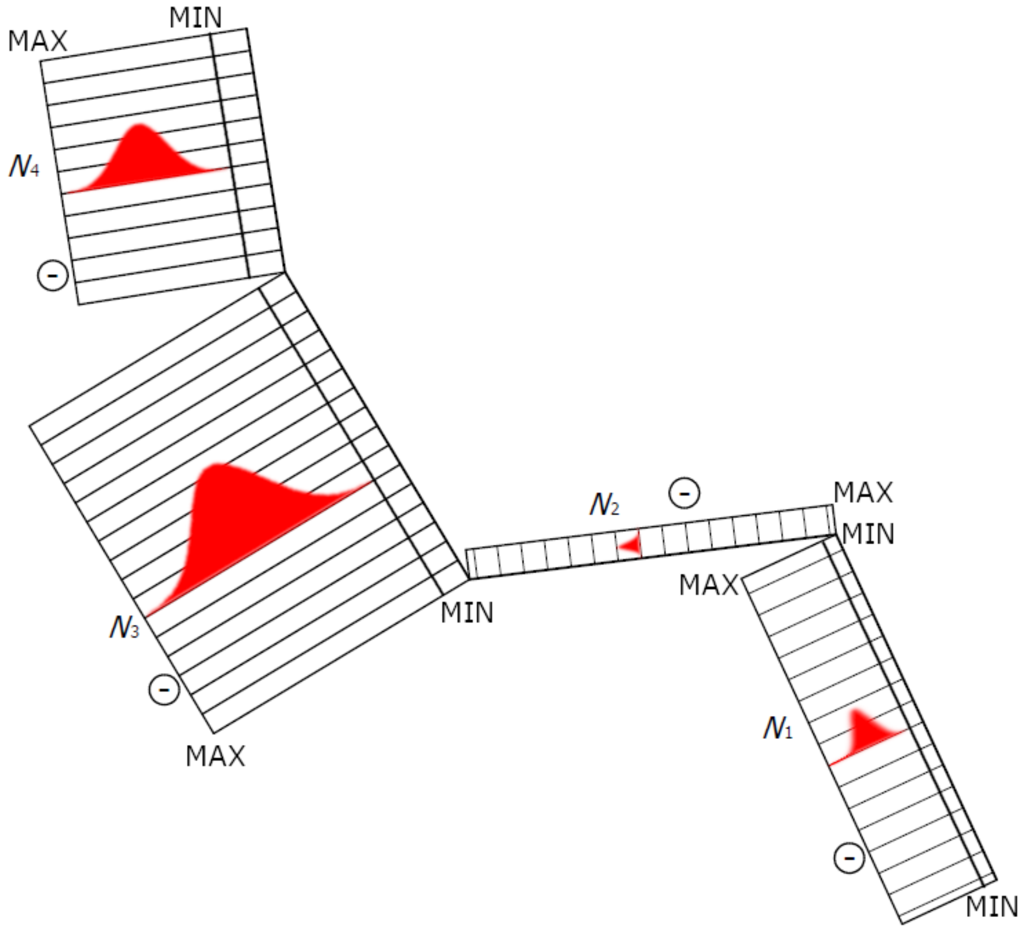

Fig. 11 Normal forces diagram with histograms

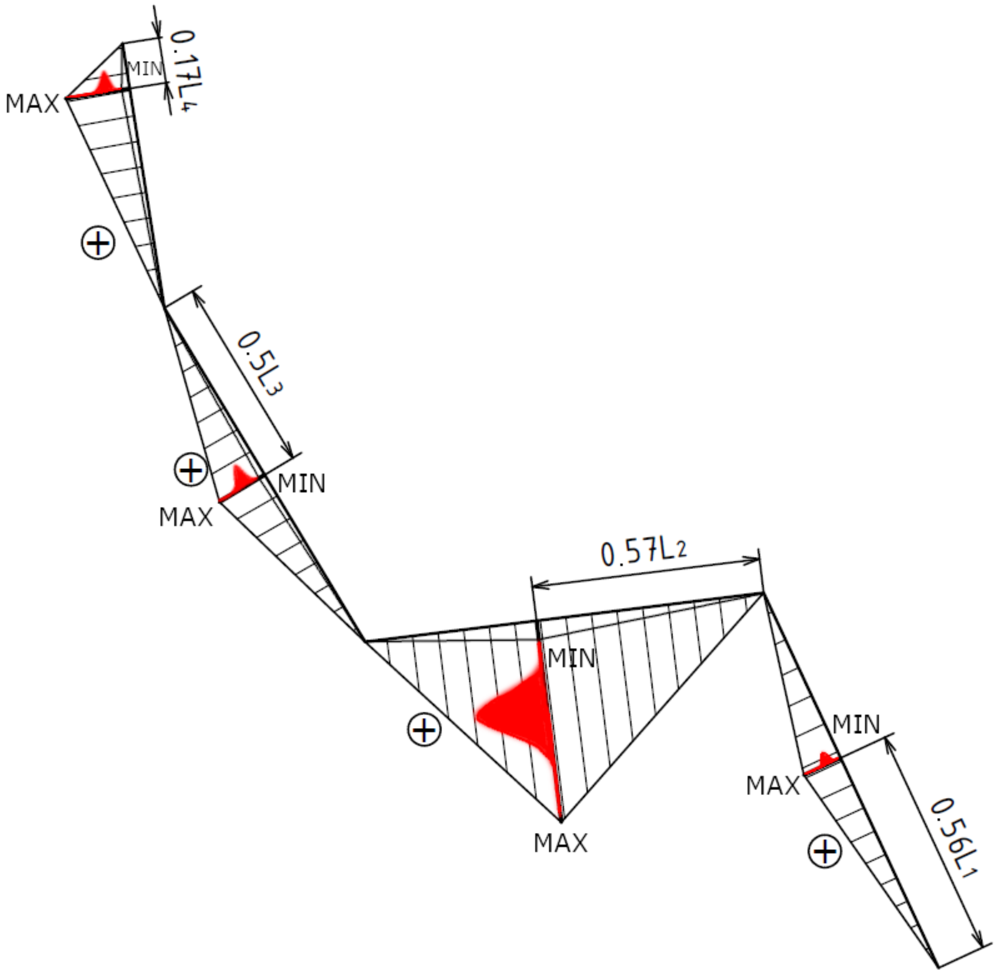

Fig. 12 Bending moments diagram with histograms

CONCLUSION

The aim of this paper is a biomechanical evaluation of the interaction between load forces to which a sitting man and the seat are exposed. All loads and dimensions given by real anthropometry (histograms with normal distribution) and are determined by direct Monte Carlo method (software Anthill). Hence, the stochastic/probabilistic approach is used.

Plane model for the stochastic solution of seat and seating man interaction was applied. This model shows sufficient biomechanical evaluation. The output data show the biggest normal force $N_{\mathrm{MAX}} = N_{3\mathrm{MAX}} = 566.7$ N in dorsum (see Graph 22 or Tab. 2). Maximum bending moment $M_{\mathrm{OMAX}} = M_{\mathrm{OMAX2}} = 46.975$ Nm is in thighs (see Graph 31 or Tab. 2), but those are not as susceptible to injury as dorsum is.

For the further calculations, shear forces and dynamic effects (e.g. by dynamic factor) could be added and finally a curvilinear or spatial (3D) model can be applied. This analysis can serve e.g. as an initial part in designing or improving chairs or as a good support for ergonomics, rehabilitation, implant design etc.

ACKNOWLEDGEMENTS

This work has been supported by The Ministry of Education, Youth and Sports of the Czech Republic from the Specific Research Project SP2019/100 & by project No. CZ.02.1.01/0.0/0.0/17_049/0008441 „Innovative therapeutic methods of musculoskeletal system in accident surgery“ (provider Operational Programme Research, Development and Education, European Union and Czech Republic).

REFERENCES

[1] https://www.slideserve.com "Population Genetics: How do Genes Move through time and Space?", [online] Available at: https://www.slideserve.com/aron/population-genetics [Accessed: 20.3.**2019**)].

[2] http://sphweb.bumc.bu.edu "The Normal Distribution: A Probability Model for a Continuous Outcome", [online] Available at: http://sphweb.bumc.bu.edu/otlt/MPH-Modules/BS/BS704_Probability/BS704_Probability8.html [Accessed: 20.3.**2019**)].

[3] Frydrýšek, K. Čepica, D., Halo, T. “Biomechanics – Simple Stochastic Model of Sitting Human”, In: Applied mechanics 2019 – Conference proceedings, Czech Republic, , pp. 32 – 37, **2019**.

[4] Čepica, D. “Biomechanics – Stochastic Loading of a Human” (unpublished bachelor thesis written in Czech language, VSB - Technical University of Ostrava, head of thesis Karel FRYDRÝŠEK), **2019**.

[5] Grepl, J., Frydrýšek, K., Penhaker, M. “A Probabilistic Model of the Interaction between a Sitting Man and a Seat”, Applied Mechanics and Materials 684, pp. 413 – 419, **2014**.

[6] Marek, P., Brozzetti, J., Guštar, M., Tikalsky, P. “Probabilistic Assessment of Structures Using Monte Carlo Simulation Background, Exercises and Software”, Prague, Czech Republic, **2003**. ISBN 80-86246-19-1

[7] Frydrýšek, K. “The probabilistic approach and its practical applications in medical and mechanical engineering”, In: Risk, Reliability and Safety: Innovating Theory and Practice - Proceedings of the 26th European Safety and Reliability Conference, ESREL 2016, United Kingdom, p. 399, **2017**.

[8] Lokaj, A., Klajmonová, K. “A probability assessment of the carrying capacity of round timber joints”, In: Advances in Civil Engineering and Building Materials IV – Selected and Peer Reviewed Papers from the 2014 4th International Conference on Civil Engineering and Building Materials, CEBM 2014, China, 2015, p. 373-378, **2015**.

[9] Konečný, P., Pustka, D. “Random variation and correlation of the weather data series - Evaluation and simulation using bounded histograms”, In: MATEC Web of Conferences – 107, Slovakia, art. No. 00085., **2017**.

[10] Frydrýšek, K., Jančo, R. “Simple planar truss (linear, nonlinear and stochastic approach)”, Strojnícky časopis – Journal of Mechanical Engineering 66 (2), pp. 5 – 12. **2016**. DOI: 10.1515/scjme-2016-0013

[11] Bažant, Z. P., Cedolin, L. “Stability of Structures: Elastic, Inelastic, Fracture, and Damage Theories”, WSPC, Singapore, **2010**. ISBN: 978-981-4317-02-3

[12] Elesztos, P., Jančo, R., Vostiar, V. “Optimization of welding process using a genetic algorithm”, Strojnícky časopis – Journal of Mechanical Engineering 68 (2), pp. 17 – 24. **2018**. DOI: 10.2478/scjme-2018-0014

[13] Enikov, E. T., Polyvas, P. P., Janco, R., Madarasz, M. “Evaluation and Testing of Novel Ocular Tactile Tonometry Device”, Mechatronics 2013: Recent Technological and scientific advances, pp. 847 – 854. **2014**. DOI: 10.1007/978-3-319-02294-9_107